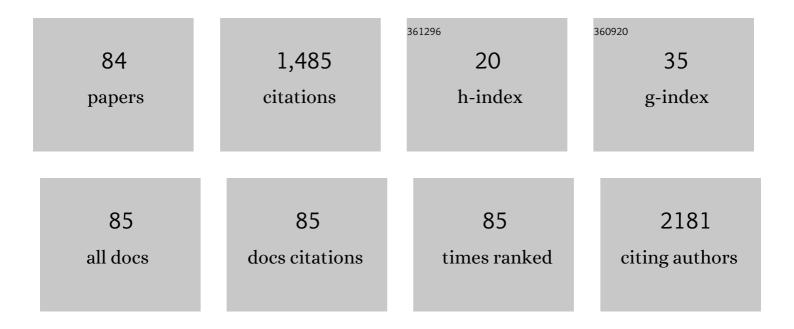
List of Publications by Year in descending order

Source: https://exaly.com/author-pdf/1592618/publications.pdf Version: 2024-02-01



#	Article	IF	CITATIONS
1	Shock wave determination of temperature dependence of twinning stress in vanadium and tantalum. Materials Science & Engineering A: Structural Materials: Properties, Microstructure and Processing, 2022, 833, 142537.	2.6	8
2	In-depth characterization of stacking faults forming during the growth of Transition-Metal Di-Chalcogenides (TMDCs) by ambient pressure-CVD. Materials Characterization, 2022, 184, 111666.	1.9	9
3	Structure solution of the Al _{69.2} Cu ₂₀ Cr _{10.8} Ï• phase. Journal of Applied Crystallography, 2022, 55, 74-79.	1.9	0
4	Influence of alloying elements and the state of order on the formation of antiphase boundaries in B2 phases. Intermetallics, 2022, 141, 107434.	1.8	4
5	Electron Diffraction Study of the Space Group Variation in the Al–Mn–Pt T-Phase. Symmetry, 2022, 14, 38.	1.1	1
6	Direct observation of initial stages of precipitation hardening process in commercial Al 6061 alloy. Journal of Materials Science, 2022, 57, 10395-10406.	1.7	1
7	Kinetics of the α-α′ phase separation in a 14%Cr oxide dispersion steel at intermediate temperatures. Materials Letters, 2021, 285, 129088.	1.3	0
8	Structural study of Al78Mn17.5Pt4.5 and (re)constitution of the Al–Mn–Pt system in its vicinity. Journal of Alloys and Compounds, 2021, 861, 158328.	2.8	3
9	Shock-induced twinning in polycrystalline vanadium: II. Surface layer. Materials Characterization, 2021, 175, 111062.	1.9	1
10	Electroplating of Pure Aluminum from [HMIm][TFSI]–AlCl3 Room-Temperature Ionic Liquid. Coatings, 2021, 11, 1414.	1.2	5
11	Deformation in nanocrystalline ceramics: A microstructural study of MgAl2O4. Acta Materialia, 2020, 183, 137-144.	3.8	27
12	Characterization of nano-sized particles in 14%Cr oxide dispersion strengthened (ODS) steel using classical and frontier microscopy methods. Materials Characterization, 2020, 160, 110075.	1.9	6
13	Novel AlCrFeNiNb0.3 high entropy alloy: Microstructure, properties and an unknown Nb-rich intermetallide. Intermetallics, 2020, 127, 106965.	1.8	10
14	Understanding the Role of the Constituting Elements of the AlCoCrFeNi High Entropy Alloy through the Investigation of Quaternary Alloys. Metals, 2020, 10, 1275.	1.0	19
15	Bonding and Stability of Ternary Structures in the CeT2Al20 (T=Ta, W, Re) and YRe2Al20 Alloys. Metals, 2020, 10, 422.	1.0	3
16	Shock wave characterization of precipitate strengthening of PH 13–8 Mo stainless steel. Acta Materialia, 2020, 187, 176-185.	3.8	13
17	Structure characterization of novel alluminides in the Nd-Re-Al system by electron crystallography methods. Materials Characterization, 2020, 168, 110562.	1.9	2
18	Explanation of structural differences and similarities between the AT ₂ Al ₁₀ phases (where A=actinide, lanthanide or rare earth element and T=transition metal). Zeitschrift Fur Kristallographie - Crystalline Materials, 2019, 234, 595-603.	0.4	2

LOUISA MESHI

#	Article	IF	CITATIONS
19	Retardation of the $\ddot{l}f$ phase formation in the AlCoCrFeNi multi-component alloy. Materials Characterization, 2019, 148, 171-177.	1.9	28
20	Characterization of Atomic Structures of Nanosized Intermetallic Compounds Using Electron Diffraction Methods. Advanced Materials, 2018, 30, e1706704.	11.1	6
21	Radiation Resistance of the U(Al, Si)3 Alloy: Ion-Induced Disordering. Materials, 2018, 11, 228.	1.3	6
22	The relation between Mn additions, microstructure and corrosion behavior of new wrought Mg-5Al alloys. Materials Characterization, 2018, 145, 101-115.	1.9	42
23	Structure and peculiarities of bonding in the Al-rich A-Mn-Al alloys (where A=Y, Gd, Th and U). Intermetallics, 2018, 100, 44-51.	1.8	5
24	Friction stir welded AM50 and AZ31 Mg alloys: Microstructural evolution and improved corrosion resistance. Materials Characterization, 2017, 126, 86-95.	1.9	33
25	Heat treatments' effects on the microstructure and mechanical properties of an equiatomic Al-Cr-Fe-Mn-Ni high entropy alloy. Materials Science & Engineering A: Structural Materials: Properties, Microstructure and Processing, 2017, 689, 384-394.	2.6	71
26	Assembly of mesoscale helices with near-unity enantiomeric excess and light-matter interactions for chiral semiconductors. Science Advances, 2017, 3, e1601159.	4.7	135
27	Long-period antiphase domains and short-range order in a B2 matrix of the AlCoCrFeNi high-entropy alloy. Scripta Materialia, 2017, 139, 49-52.	2.6	65
28	Nanometric diamond delta doping with boron. Physica Status Solidi - Rapid Research Letters, 2017, 11, 1600329.	1.2	27
29	Ordered U(Al, Si)3 phase: Structure and bonding. Journal of Alloys and Compounds, 2017, 690, 884-889.	2.8	7
30	Structure of <i>A</i> – <i>T</i> –Al aluminides (<i>A</i> = actinide/lanthanide; <i>T</i> = transition) Tj ETQq	0.0 _{0.0} gBT	/Oyerlock 10
31	Electrochemical Intercalation of Lithium Ions into NbSe ₂ Nanosheets. ACS Applied Materials & Interfaces, 2016, 8, 11390-11395.	4.0	56
32	Effect of oxygen pressure on structure and ionic conductivity of epitaxial Li _{0.33} La _{0.55} TiO ₃ solid electrolyte thin films produced by pulsed laser deposition. RSC Advances, 2016, 6, 61974-61983.	1.7	21
33	Refinement of the Al-rich part of the Al–Cu–Re phase diagram and atomic model of the ternary Al6.2Cu2Re phase. Journal of Alloys and Compounds, 2016, 670, 18-24.	2.8	4
34	Crystal structure of the Th 2 Ni 10 Al 15 phase solved using electron diffraction tomography. Journal of Alloys and Compounds, 2016, 660, 496-502.	2.8	6
35	Structural changes as a function of transition metal's (T) type in the ThT2Al20 alloys. Acta Crystallographica Section A: Foundations and Advances, 2016, 72, s236-s236.	0.0	0
36	A study of the Al–Pt–Ir phase diagram. Journal of Alloys and Compounds, 2015, 646, 873-878.	2.8	6

#	Article	IF	CITATIONS
37	Combinatorial synthesis and high-throughput characterization of the thin film materials system Co-Mn-Ge: Composition, structure, and magnetic properties. Physica Status Solidi (A) Applications and Materials Science, 2015, 212, 1969-1974.	0.8	9
38	New Nanocrystalline Materials: A Previously Unknown Simple Cubic Phase in the SnS Binary System. Nano Letters, 2015, 15, 2174-2179.	4.5	126
39	Addressing the issue of precipitates in maraging steels – Unambiguous answer. Materials Science & Engineering A: Structural Materials: Properties, Microstructure and Processing, 2015, 638, 232-239.	2.6	63
40	Elastic consideration of the precipitation in model alloys of maraging steels: theory and experimental validation. Journal of Materials Science, 2015, 50, 4970-4979.	1.7	18
41	Abrupt symmetry decrease in the ThT2Al20 alloys (TÂ=Â3d transition metal). Journal of Alloys and Compounds, 2015, 648, 353-359.	2.8	14
42	Formation of Complex Intermetallics in the Al-Rich Part of Al-Pt-Ru. Journal of Phase Equilibria and Diffusion, 2015, 36, 327-332.	0.5	7
43	Sensitivity of thermo-electric power measurements to α–α′ phase separation in Cr-rich oxide dispersion strengthened steels. Journal of Materials Science, 2015, 50, 4629-4635.	1.7	8
44	Thermodynamic modeling of Al–U–X (X = Si,Zr). Journal of Nuclear Materials, 2015, 464, 170-184.	1.3	19
45	Characterization of new aluminides found in the ThT2Al2O alloys (where T = Ti, V, Mn). Journal of Alloys and Compounds, 2015, 641, 1-6.	2.8	19
46	Addressing a "Black Box―of Bottom-Up Synthesis: Revealing the Structures of Growing Colloidal-Nanocrystal Nuclei. Inorganic Chemistry, 2015, 54, 10521-10523.	1.9	1
47	The origin of the effect of aging on the thermoelectric power of maraging C250 steel. Journal of Materials Science, 2015, 50, 7698-7704.	1.7	2
48	Increased corrosion resistance of the AZ80 magnesium alloy by rapid solidification. Journal of Biomedical Materials Research - Part B Applied Biomaterials, 2015, 103, 1541-1548.	1.6	14
49	Crystal structures of the Al–Ti–Pt τ5 and τ6 phases solved by zonal precession electron diffraction. Journal of Alloys and Compounds, 2015, 621, 47-52.	2.8	6
50	Atomic structure solution of the complex quasicrystal approximant Al ₇₇ Rh ₁₅ Ru ₈ from electron diffraction data. Acta Crystallographica Section B: Structural Science, Crystal Engineering and Materials, 2014, 70, 999-1005.	0.5	13
51	New ordered phase in the quasi-binary UAl ₃ –USi ₃ system. Acta Crystallographica Section B: Structural Science, Crystal Engineering and Materials, 2014, 70, 580-585.	0.5	11
52	Strategies for full structure solution of intermetallic compounds using precession electron diffraction zonal data. Journal of Applied Crystallography, 2014, 47, 1032-1041.	1.9	6
53	A study of the Al–Pd–Pt alloy system. Journal of Alloys and Compounds, 2014, 600, 125-129.	2.8	7
54	Study of ternary complex Al—Mg—Ag intermetallides using Precession Electron Diffraction. Zeitschrift Fur Kristallographie - Crystalline Materials, 2013, 228, 59-62.	0.4	2

#	Article	IF	CITATIONS
55	Characterization of structural defects in highly mismatched GaP nanowires. Materials Letters, 2013, 113, 38-41.	1.3	0
56	Evaluation of microstructural damage and alteration of polytypes to determine the aging of silicon carbide. , 2013, , .		0
57	Microstructural Evolution of Cr-Rich ODS Steels as a Function of Heat Treatment at 475°C. Metallography, Microstructure, and Analysis, 2012, 1, 158-164.	0.5	8
58	Regioselective placement of alkanethiolate domains on tetrahedral and octahedral gold nanocrystals. Chemical Communications, 2012, 48, 9765.	2.2	14
59	Orientations of polyoxometalate anions on gold nanoparticles. Dalton Transactions, 2012, 41, 9849.	1.6	20
60	Crystal structure of a new quaternary Mg–Zn–Ca–Li phase. Intermetallics, 2012, 22, 62-67.	1.8	4
61	A study of the Al-rich part of the Al–Ni–Pt alloy system. Journal of Alloys and Compounds, 2012, 514, 60-63.	2.8	13
62	Polyoxometalate-directed assembly of water-soluble AgCl nanocubes. Chemical Communications, 2012, 48, 2207.	2.2	12
63	Friction, wear and structure of Cu samples in the lubricated steady friction state. Tribology International, 2012, 46, 154-160.	3.0	22
64	New orthorhombic phase in U–Fe–Al–Si system. Journal of Alloys and Compounds, 2011, 509, 206-209.	2.8	5
65	New complex intermetallic in the Al–Rh–Ru alloy system. Journal of Alloys and Compounds, 2011, 509, 6551-6555.	2.8	11
66	An investigation of the Al–Rh–Ru phase diagram above 50at.% Al. Journal of Alloys and Compounds, 2011, 509, 8018-8021.	2.8	8
67	Why UFexAl12â^'x phase does not crystallize with ThMn12-structure type, when xÂ=Â2?. Intermetallics, 2011, 19, 713-720.	1.8	11
68	Dislocation structure and hardness of surface layers under friction of copper in different lubricant conditions. Acta Materialia, 2011, 59, 342-348.	3.8	38
69	GaN devices based on nanorods. Journal of Physics: Conference Series, 2010, 209, 012001.	0.3	6
70	Size-dependent spin state and ferromagnetism in La0.8Ca0.2CoO3 nanoparticles. Journal of Applied Physics, 2010, 108, 063907.	1.1	17
71	Liquidus projection of Al-rich corner of the ternary Al–Fe–U system. Intermetallics, 2010, 18, 2119-2123.	1.8	2
72	Crystal structure of the Al2Culr phase. Journal of Alloys and Compounds, 2010, 496, 208-211.	2.8	3

#	Article	IF	CITATIONS
73	Identification of a new hexagonal phase in the Al–Cu–Re system. Journal of Alloys and Compounds, 2009, 488, 108-111.	2.8	5
74	Self-Assembly and Structure of Directly Imaged Inorganic-Anion Monolayers on a Gold Nanoparticle. Journal of the American Chemical Society, 2009, 131, 17412-17422.	6.6	102
75	The reduction of threading dislocations in GaN using a GaN nanocolumn interlayer. Physica Status Solidi C: Current Topics in Solid State Physics, 2008, 5, 1645-1647.	0.8	8
76	Defect-controlled growth of GaN nanorods on (0001)sapphire by molecular beam epitaxy. Applied Physics Letters, 2008, 93, 111911.	1.5	24
77	Direct Imaging of the Ligand Monolayer on an Anion-Protected Metal Nanoparticle through Cryogenic Trapping of its Solution-State Structure. Journal of the American Chemical Society, 2008, 130, 16480-16481.	6.6	45
78	Determination of the structure of a new tetragonal U2FeAl20 phase. Journal of Alloys and Compounds, 2008, 460, 196-200.	2.8	4
79	Defect reduction in GaN/(0001)sapphire films grown by molecular beam epitaxy using nanocolumn intermediate layers. Applied Physics Letters, 2008, 92, .	1.5	63
80	Nano-pendeo GaN Growth of Light Emitting Devices on Silicon. Journal of Light and Visual Environment, 2008, 32, 187-190.	0.2	1
81	Tetragonal phase in Al-rich region of U–Fe–Al system. Journal of Alloys and Compounds, 2005, 402, 84-88.	2.8	9
82	The structure of the ternary aluminide ThFe2Al10. Intermetallics, 2005, 13, 792-795.	1.8	13
83	Determination of the structure of UFe2Al10 compound. Journal of Alloys and Compounds, 2004, 370, 206-210.	2.8	19
84	Identification of the structure of a new Al–U–Fe phase by electron microdiffraction technique. Journal of Alloys and Compounds, 2002, 347, 178-183.	2.8	21